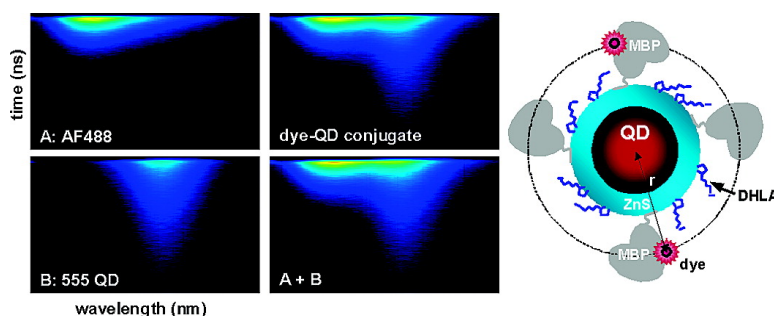


Can Luminescent Quantum Dots Be Efficient Energy Acceptors with Organic Dye Donors?

Aaron R. Clapp, Igor L. Medintz, Brent R. Fisher, George P. Anderson, and Hedi Mattoussi

J. Am. Chem. Soc., **2005**, 127 (4), 1242-1250 • DOI: 10.1021/ja045676z • Publication Date (Web): 06 January 2005

Downloaded from <http://pubs.acs.org> on March 24, 2009



More About This Article

Additional resources and features associated with this article are available within the HTML version:

- Supporting Information
- Links to the 20 articles that cite this article, as of the time of this article download
- Access to high resolution figures
- Links to articles and content related to this article
- Copyright permission to reproduce figures and/or text from this article

[View the Full Text HTML](#)

Can Luminescent Quantum Dots Be Efficient Energy Acceptors with Organic Dye Donors?

Aaron R. Clapp,[†] Igor L. Medintz,[‡] Brent R. Fisher,[§] George P. Anderson,[‡] and Hedi Mattoussi^{*†}

Contribution from the U.S. Naval Research Laboratory, Optical Sciences Division, Code 5611, Washington, D.C. 20375; U.S. Naval Research Laboratory, Center for Bio/Molecular Science and Engineering, Code 6900, Washington, D.C. 20375; and Massachusetts Institute of Technology, Department of Chemistry, Cambridge, Massachusetts 02139

Received July 19, 2004; E-mail: hedimat@ccs.nrl.navy.mil

Abstract: We assessed the ability of luminescent quantum dots (QDs) to function as energy acceptors in fluorescence resonance energy transfer (FRET) assays, with organic dyes serving as donors. Either AlexaFluor 488 or Cy3 dye was attached to maltose binding protein (MBP) and used with various QD acceptors. Steady-state and time-resolved fluorescence measurements showed no apparent FRET from dye to QD. We attribute these observations to the dominance of a fast radiative decay rate of the donor excitation relative to a slow FRET decay rate. This is due to the long exciton lifetime of the acceptor compared to that of the dye, combined with substantial QD direct excitation.

Introduction

Fluorescence resonance energy transfer (FRET) is a powerful technique for probing very small (sub-nanometer scale) changes in the separation distance between donor and acceptor fluorophores, which is ideal for the sensitive detection of molecular binding events and changes in protein conformation in response to interactions with a particular target molecule or to changes in the solution environment.^{1–3} Recently, we have employed hydrophilic (water soluble) CdSe–ZnS core–shell nanocrystals to demonstrate that QDs are excellent FRET donors with proximal organic dyes.^{4–6} The broad excitation spectra and large absorption cross section of QDs paired with the narrow excitation spectra of acceptor dyes permit excitation at the dye absorption minimum which allows efficient FRET while significantly reducing unwanted direct excitation of the acceptor. In these studies, aggregate-free compact QD bioconjugates were formed in solution by immobilizing dye-labeled proteins onto the surface of QDs using a self-assembly process driven by metal-affinity coordination.^{4,5,8} Because a single QD can ac-

commodate several proteins on its surface (colloidal QDs have dimensions comparable to those of proteins), it is possible to increase the number of dye-labeled proteins in a QD bioconjugate and enhance the FRET efficiency significantly. This strategy was implemented by our group in designing a homogeneous solution phase FRET-based sensing assembly for the detection of the nutrient sugar maltose.⁵ In this sensor design we utilized *E. coli* maltose binding protein (MBP), which binds preferentially to maltose.⁷ MBP was self-assembled on the QD surface and was preloaded with an analogue substrate conjugated to a QSY9 quencher dye (β -cyclodextrin-QSY9), resulting in a substantial quenching of the QD photoluminescence (PL) due to FRET from the QD to the proximal quencher. Adding maltose to the sample displaced the β -cyclodextrin-QSY9 transducing agent, resulting in recovery of QD PL in a systematic and concentration-dependent manner.⁵ We also found that by placing several active dye-labeled proteins around the QD center, the overall FRET signal was improved substantially over a simple one donor-to-one acceptor FRET pair.⁴ More recently, we complemented the above findings with an investigation of the conformation of the protein self-assembled on the nanocrystal surface, using FRET between a QD donor interacting with an acceptor whose location in the MBP amino acid sequence was precisely controlled to estimate the separation distance of those sequences from the donor center.⁹ This provided a critically important understanding of how bioreceptors, especially proteins, orient themselves around the nanoparticle surface in the present self-assembly process.

[†] U.S. Naval Research Laboratory, Optical Sciences Division.

[‡] U.S. Naval Research Laboratory, Center for Bio/Molecular Science and Engineering.

[§] Massachusetts Institute of Technology.

- (1) Iqbal, S. S.; Mayo, M. W.; Bruno, J. G.; Bronk, B. V.; Batt, C. A.; Chambers, J. P. *Biosens. Bioelectron.* **2000**, *15*, 549–578.
- (2) (a) Lakowicz, J. R. *Principles of Fluorescence Spectroscopy*, 2nd ed.; Kluwer Academic: New York, 1999. (b) Lakowicz, J. R.; Piszczek, G.; Kang, J. S. *Anal. Biochem.* **2000**, *288*, 62–75.
- (3) Jares-Erijman, E. A.; Jovin, T. M. *Nat. Biotechnol.* **2003**, *21*, 1387–1395.
- (4) Clapp, A. R.; Medintz, I. L.; Mauro, J. M.; Fisher, B. R.; Bawendi, M. G.; Mattoussi, H. *J. Am. Chem. Soc.* **2004**, *126*, 301–310.
- (5) Medintz, I. L.; Clapp, A. R.; Mattoussi, H.; Goldman, E. R.; Fisher, B. M.; Mauro, J. M. *Nat. Mater.* **2003**, *2*, 630–638.
- (6) Tran, P. T.; Goldman, E. R.; Anderson, G. P.; Mauro, J. M.; Mattoussi, H. *Phys. Status Solidi B* **2002**, *229*, 427–432.
- (7) Medintz, I. L.; Goldman, E. R.; Lassman, M. E.; Mauro, J. M. *Bioconjugate Chem.* **2003**, *14*, 909–918.

- (8) Goldman, E. R.; Medintz, I. L.; Hayhurst, A.; Anderson, G. P.; Mauro, J. M.; Iverson, B. L.; Georgiou, G.; Mattoussi, H. *Anal. Chim. Acta*, in press.
- (9) Medintz, I. L.; Konert, J. H.; Clapp, A. R.; Stanish, I.; Twigg, M. E.; Mattoussi, H.; Mauro, J. M.; Deschamps, J. R. *Proc. Nat. Acad. Sci. (PNAS)* **2004**, *101*, 9612–9617.

Other groups have also reported the use of QDs as energy donors in FRET-based studies to either detect conjugate formation or investigate the replication and telomerization of surface bound DNA segments.^{10,11} While these studies have shown that QDs can function effectively as energy donors in FRET-based assays, inorganic fluorophores may also be superior energy acceptors. QDs have large extinction coefficients (typically about 5–10 times larger than most dyes) that extend over a broad range of wavelengths.¹² In contrast, organic dyes are of molecular dimensions and have relatively high photoluminescence quantum yields (QYs). Based on predictions of the Förster formalism, if dyes are able to donate energy to QD acceptors, efficient FRET should be achieved in QD–dye-labeled protein complexes.² Furthermore, a configuration where a single QD is conjugated to several dye-labeled proteins should also permit one to achieve efficient FRET, as demonstrated in our previous investigations where QDs functioned as efficient energy donors.^{4–6,9} Using the naturally occurring UV absorption and fluorescence of tryptophan (Trp) and its abundance in a variety of biomolecules, Mamedova et al. reported observation of a substantial energy transfer between BSA (bovine serum albumin which contains two tryptophan residues) and CdTe QDs in a BSA–QD conjugate.¹³ In particular, the authors reported that exciting BSA–QD conjugates, assembled using a glutaraldehyde linker with a presumably two BSA per QD ratio, at 290 nm resulted in substantial FRET between the Trp and QD, manifesting in a loss of BSA emission at 340 nm and about 2-fold gain in the emission of the QD acceptor.¹³ In an interesting recent report, Acherman et al. reported efficient nonradiative energy transfer in a three-layer heterostructure between a 3 nm quantum well (QW) donor layer made of InGaN and a thin layer made of colloidal QDs processed from organic solutions, separated from the donor layer (QW) by a 2 nm n-type GaN capping layer.¹⁴ The authors have further shown that in this structure with 2-D symmetry the FRET efficiency varied as the inverse fourth power of the separation distance ($E \approx 1/d^4$). They attributed their observations to a sufficiently fast energy transfer rate compared with the radiative decay rate of the QW excitation energy.

Luminescent QDs made from II–VI and III–V semiconductor materials can be synthesized to emit over a wide region of the optical spectrum from the visible spectrum into the near-infrared, which is ideal for applications such as signal multiplexing^{15,16} and in vivo cellular and tissue imaging.^{17–21} Advances in designing versatile routes to prepare robust

nanocrystals and implementing a variety of surface functionalization techniques to exchange the surface capping ligands have allowed colloidal QDs to be dispersed in aqueous solutions and to be conjugated to a variety of biomolecules.^{18–25}

In the present study, we used our previously developed QD–dye-labeled protein conjugates to explore the FRET properties in a “reverse” format, where a set of energy donating organic dyes are arrayed quasi-symmetrically around a central QD energy acceptor. The organic dyes are covalently attached at a specific residue of an engineered maltose binding protein (MBP). Dye-labeled MBP is allowed to self-assemble around the QD surface through coordination of the C-terminal pentahistidine tail with zinc metal on the QD surface. The ratio of dye-labeled protein was varied while maintaining a fixed total number of proteins per QD. Steady-state fluorescence spectra were collected from the QD–dye-labeled protein conjugates along with the spectra of the individual donor and acceptor species as direct excitation controls. Using a set of three dye–QD pairs with substantial spectral energy overlap (AlexaFluor 488 and 555 nm emitting QDs, AlexaFluor 488 and 570 nm emitting QDs, and Cy3 and 590 nm emitting QDs; see Figure 1) and varying the ratio between dye and QDs from 1 to 10, we found *no evidence of FRET* between these dyes and the central QD. Additional time-resolved fluorescence experiments have further confirmed these findings. We also tested the ability of the amino acid Trp to transfer excitation energy nonradiatively to CdSe–ZnS QDs using our MBP–QD conjugate configuration of 15 proteins per nanocrystal (no organic dyes present). This presents an additional favorable and sensitive system to test FRET, due to the relatively large number of Trp residues in each conjugate (120 Trp units per QD conjugate, with 8 residues per MBP). These conjugates were excited at 280 nm (where both Trp and QDs absorb) and at longer wavelengths where only the QD absorbs. We saw no evidence of FRET between the Trp donor and QDs.

We attribute these observations to the dominance of a fast radiative decay rate of the dye donor excitation energy relative to an extremely slow nonradiative FRET decay rate, in the presence of a QD acceptor; the QD acceptor has a longer exciton radiative lifetime than the dye donor. In addition, because of their broad absorption, QD acceptors are also efficiently excited along with the dyes, which could imply that Auger recombination can further reduce the probability of additional excitation via energy transfer.^{26,27} This rationale was tested using a metal chelate ruthenium dye with a reported long phosphorescence lifetime (~350 ns). The dye was attached to MBP at a specific residue, and time-resolved fluorescence experiments were used to measure changes in the excitation lifetimes of the fluorophores on MBP–dye conjugated to 610 nm emitting QDs. Preliminary data indicate that a substantial rate of FRET could be measured,

- (10) Willard, D. M.; Carillo, L. L.; Jung, J.; Van Orden, A. *Nano Lett.* **2001**, *1*, 469–474.
- (11) Patolsky, F.; Gill, R.; Weizmann, Y.; Mokari, T.; Banin, U.; Willner, I. *J. Am. Chem. Soc.* **2003**, *125*, 13918–13919.
- (12) Leatherdale, C. A.; Woo, W.-K.; Mikulec, F. V.; Bawendi, M. G. *J. Phys. Chem. B* **2002**, *106*, 7619–7622.
- (13) Mamedova, N. N.; Kotov, N. A.; Rogach, A. L.; Studer, J. *Nano Lett.* **2001**, *1*, 281–286.
- (14) Achermann, M.; Petruska, M. A.; Kos, S.; Smith, D. L.; Koleske, D. D.; Klimov, V. I. *Nature* **2004**, *429*, 642–646.
- (15) Lacoste, T. D.; Michalet, X.; Pinaud, F.; Chemla, D. S.; Alivisatos, A. P.; Weiss, S. *Proc. Nat. Acad. Sci. U.S.A.* **2000**, *97*, 9761–9766.
- (16) Goldman, E. R.; Clapp, A. R.; Anderson, G. P.; Uyeda, H. T.; Mauro, J. M.; Medintz, I. L.; Mattoussi, H. *Anal. Chem.* **2004**, *76*, 684–688.
- (17) Bruchez, M.; Moronne, M.; Gin, P.; Weiss, S.; Alivisatos, A. P. *Science* **1998**, *281*, 2013–2015.
- (18) Dubertret, B.; Skourides, P.; Norris, D. J.; Noireaux, V.; Brivanlou, A. H.; Libchaber, A. *Science* **2002**, *298*, 1759–1762.
- (19) Wu, X.; Liu, H.; Liu, J.; Haley, K. N.; Treadway, J. A.; Larson, J. P.; Ge, N.; Peale, F.; Bruchez, M. P., Jr. *Nat. Biotechnol.* **2003**, *21*, 41–46.
- (20) Jaiswal, J. K.; Mattoussi, H.; Mauro J. M.; Simon, S. M. *Nat. Biotechnol.* **2003**, *21*, 47–51.

- (21) Kim, S.; Lim, Y. T.; Soltesz, E. G.; De Grand, A. M.; Lee, J.; Nakayama, A.; Parker, J. A.; Mihaljevic, T.; Laurence, R. G.; Dor, D. M.; Cohn, L. H.; Bawendi M. G.; Frangioni, J. V. *Nat. Biotechnol.* **2004**, *22*, 93–97.
- (22) Chan, W. C. W.; Nie, S. *Science* **1998**, *281*, 2016–2018.
- (23) Mattoussi, H.; Mauro, J. M.; Goldman, E. R.; Anderson, G. P.; Sundar, V. C.; Mikulec, F. V.; Bawendi, M. G. *J. Am. Chem. Soc.* **2000**, *122*, 12142–12150.
- (24) Mattoussi, H.; Kuno, M. K.; Goldman, E. R.; Anderson, G. P.; Mauro, J. M. *Optical Biosensors: Present and Future*; Elsevier: The Netherlands, 2002; pp 537–569.
- (25) Kim, S.; Bawendi, M. G. *J. Am. Chem. Soc.* **2003**, *125*, 14652–14653.
- (26) Chepic, D. J.; Efros, A. I.; Ekimov, A. I.; Ivanov, M. G.; Kharchenko, V. I.; Kudriatsev, I. A.; Yazeva, T. V. *J. Lumin.* **1990**, *47*, 113–127.
- (27) Klimov V. I.; Mikhailovsky A. A.; McBranch D. W.; Leatherdale C. A.; Bawendi, M. G. *Science* **2000**, *287*, 1011–1013.

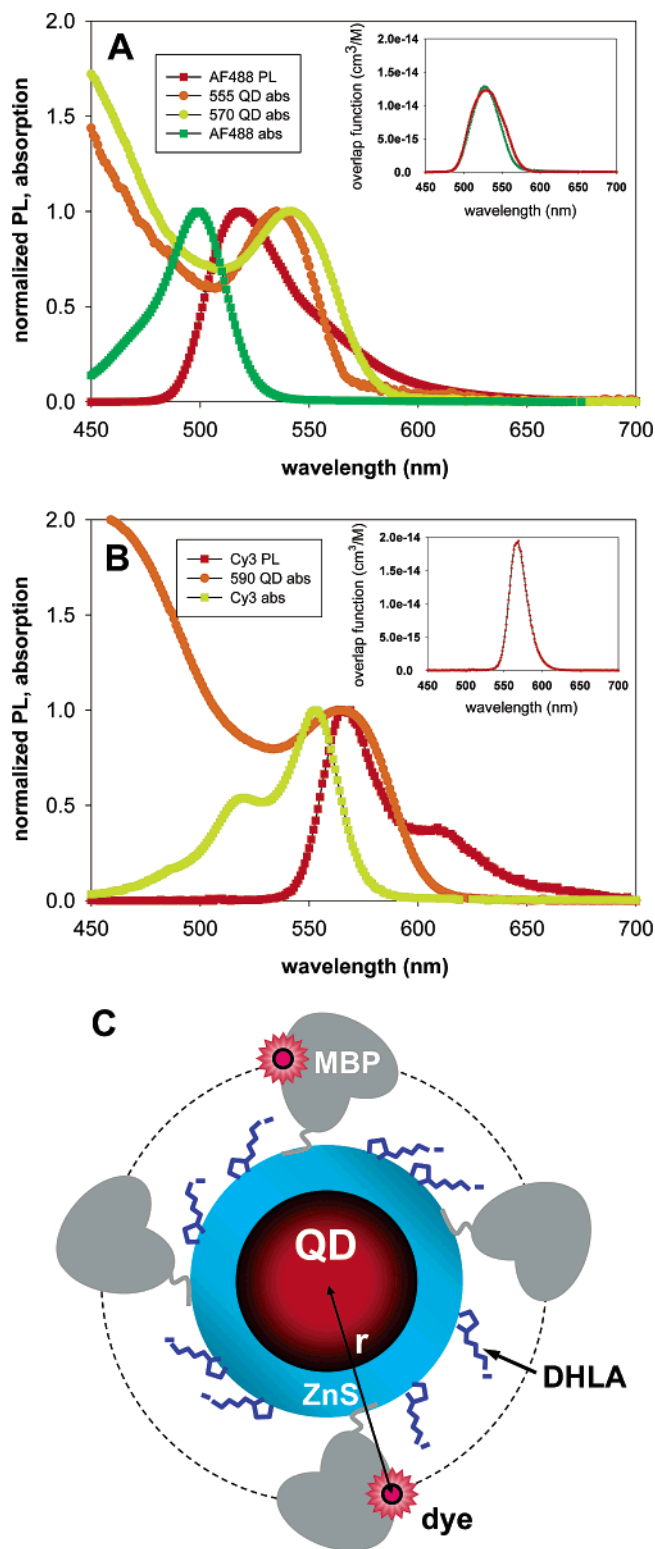


Figure 1. Plots of the QD absorption together with the normalized absorption and PL spectra of dye for the three sets of donor–acceptors used. Inserts show the overlap functions defined as $J(\lambda) = PL_{D-corr}(\lambda) \times \lambda^4 \times \epsilon_A(\lambda)$, plotted versus wavelength, where PL_{D-corr} and ϵ_A , respectively, designate the normalized donor photoemission and the acceptor extinction coefficient spectra. (A) Spectra of AlexaFluor 488 (donor), 555, and 570 nm emitting QDs (acceptors). (B) Spectra of Cy3 (donor) and 590 nm emitting QDs (acceptor). According to Förster theory, each pair has sufficient spectral overlap for significant FRET efficiency. (C) Schematic representation of the QD–dye-labeled protein conjugate used (not to scale).

confirming the importance of the relative donor acceptor lifetimes for realizing nonradiative energy transfer to luminescent QD acceptors.

Materials and Methods

Quantum Dot Synthesis. Populations of CdSe–ZnS core–shell QDs (having PL emission maxima at 515, 555, 570, 590, and 610 nm) were prepared using documented synthetic techniques consisting of growth and annealing of organometallic precursors at high temperature.^{28–31} The resulting CdSe–ZnS core–shell QDs were rendered water-soluble by replacing the native hydrophobic TOP/TOPO organic capping ligand with dihydrolipoic acid (DHLA).²³ The DHLA-capped QDs are uniformly negatively charged due to the deprotonated carboxylic acid end groups and are exceptionally stable in basic buffer solutions (pH 7.5–10).^{4,23}

Maltose Binding Protein. Maltose binding protein was engineered to express a C-terminal pentahistidine sequence to promote coordination with the Zn ions on the QD surface.^{4,5,9,32} In this study, we labeled MBP with either AlexaFluor 488 (AF488) or Cy3 dye at a unique residue (Cys95). The protein was reduced with dithiothreitol (Pierce, Rockford, IL) and mixed with monofunctional maleimide-Cy3 (Amersham Pharmacia, Piscataway, NJ) or AlexaFluor 488 (Molecular Probes, Eugene, OR). This procedure permitted an average labeling ratio of 1.0 dye/MBP, as deduced from the extinction coefficients of the protein at 280 nm and at the maximum absorption of the dye (492 nm for AF488 and 553 nm for Cy3, see Figure 1). Dye-labeled MBP proteins were purified by column chromatography using PD-10 columns (Amersham Pharmacia) to remove excess free dye.

QD–Protein Conjugate Preparation. We have previously shown that histidine-terminated MBP binds tightly onto DHLA-capped CdSe–ZnS core–shell QDs.^{4,5} This is routinely verified by the progressive enhancement of the MBP–QD conjugate QY as the number of surface-conjugated proteins increases.^{5,23} A working solution of proteins was first prepared by adding proportional amounts of dye-labeled and unlabeled MBP to 100 μL (total volume) of 10 mM sodium tetraborate buffer (pH 9.5). DHLA-capped QDs were added to the MBP solution and allowed to self-assemble for 15–20 min at room temperature. Molar ratios of MBP–dye to QDs were discretely varied among samples from 0 to 10 while the overall ratio of MBP (labeled and unlabeled) to QD was maintained at 15:1. This QD–protein configuration was used for all samples. The individual samples were then diluted with sodium tetraborate buffer to a total volume of 3 mL. This method allowed accurate control over the conjugate configuration and the number of proteins immobilized on each QD–protein assembly.⁵ Solutions were placed in a 10 mm optical path quartz fluorescence cuvette (Spectrocell, Oreland, PA) and the emission spectra (steady-state fluorescence) were collected using a SPEX Fluorolog-2 fluorimeter (Jobin Yvon/SPEX, Edison, NJ). Samples using AF488 were excited at 450 nm, whereas samples using Cy3 were excited at 520 nm. Excitation wavelengths for both systems were chosen near the absorption peaks of the dyes to maximize excitation of the donor molecules with respect to the QD acceptor and reduce direct excitation of the QD acceptor. The range of concentrations used in our study was below the threshold of significant inner filtering effects.

Fluorescence Lifetime Measurements. Fluorescence lifetimes were measured using a custom-built far-field epifluorescence microscope coupled to a spectrometer and time-gated intensified charge-coupled device (CCD) camera (Imager QE, LaVision GmbH, Göttingen, Germany). The excitation light source was coupled to the microscope

- (28) Murray, C. B.; Norris, D. J.; Bawendi, M. G. *J. Am. Chem. Soc.* **1993**, *115*, 8706–8715.
 (29) Hines, M. A.; Guyot-Sionnest, P. *J. Phys. Chem. B* **1996**, *100*, 468–471.
 (30) Dabbousi, B. O.; Rodriguez-Viejo, J.; Mikulec, F. V.; Heine, J. R.; Mattoussi, H.; Ober, R.; Jensen, K. J.; Bawendi, M. G. *J. Phys. Chem. B* **1997**, *101*, 9463–9475.
 (31) Qu, L.; Peng, Z. A.; Peng, X. *Nano Lett.* **2001**, *1*, 333–337.
 (32) Medintz, I. L.; Trammel, S. A.; Mattoussi, H.; Mauro, J. M. *J. Am. Chem. Soc.* **2004**, *126*, 30–31.

collection axis using a 400 nm dichroic filter, and a 0.3 NA 10× objective (Nikon, Tokyo, Japan), placed after the dichroic filter, was used to focus the excitation light onto the sample and collect the emitted fluorescence signal. An additional long pass filter inserted after the dichroic mirror was used to eliminate residual signal from the laser line and transmit only relevant photoemission signals onto the CCD detector. A pulsed GaN diode laser (414 nm, 5 MHz, 90 ps full width at half-maximum, Model LDH400, PicoQuant GmbH, Berlin, Germany) was used to excite the sample. Data were collected at room temperature using a 4 mm optical path fluorescence cell filled with 0.5 mL of QD-conjugates in buffer solution, as described above. Raw intensity data were obtained and analyzed as functions of time and wavelength using DaVis software (LaVision GmbH).⁴

Results and Discussion

Steady-State Fluorescence Measurements. Figure 1 shows plots of QD absorption along with normalized absorption and photoluminescence of the dye for the three sets of donor–acceptor used. The overlap function defined as $J(\lambda) = \text{PL}_{\text{D-corr}}(\lambda) \times \lambda^4 \times \epsilon_{\text{A}}(\lambda)$ are shown in the inserts, where $\text{PL}_{\text{D-corr}}$ and ϵ_{A} , respectively, designate the normalized donor photoemission and the acceptor extinction coefficient spectra. There is substantial energy overlap for FRET in all cases explored. Figure 2A–C show the PL spectra after deconvolution for an increasing number of dye-labeled proteins in each MBP–QD conjugate for the three sets of dye–QD pairs investigated: AF488 donor and 555 nm QD acceptor, AF488 donor and 570 nm QD acceptor, and Cy3 donor and 590 nm QD acceptor. The composite photoemission spectra were deconvoluted assuming a linear superposition of signals to derive fluorescence contribution characteristic of the individual dye and QD fluorophores. The deconvoluted spectra show that there is no measurable change in either donor PL (no dye PL loss) or the QD acceptor PL (no QD PL gain) upon formation of the QD–dye-labeled protein conjugate. Increasing the fraction of labeled MBP in the conjugate, which should have increased the overall rate of energy transfer to the acceptor, did not translate into an increase in the QD PL signal.

Figure 3 shows the PL spectra of MBP–QD conjugates (without dye label present) excited at 280 nm (where both Trp and QD absorb), at 340 nm, and at 400 nm (where only the nanocrystal should absorb and thereby contribute to the PL signal). Emission spectra of QD-only solutions were also collected (as controls) to account for the known effects of PL enhancement due to simple QD–protein conjugation, as previously reported.^{4,5,23,33} Further, we employed smaller size QDs with emission centered around 515 nm to avoid any possible interference from the second optical overtone (generated by the diffraction grating in the spectrograph) at 560 nm when a 280 nm excitation line is used.³⁴ With this system we do not see any measurable FRET between the Trp residues within MBP and the CdSe–ZnS QD used in our QD–protein conjugates. When exciting at 400 nm, only emission from the QD is observed. However, when exciting at 280 nm we collect emission from both MBP and QDs but the enhancement in the QD emission (observed for excitation at 280 nm) is commensurate with the increase in its absorption at 280 nm compared to that at 400 nm. Exciting the protein only produced

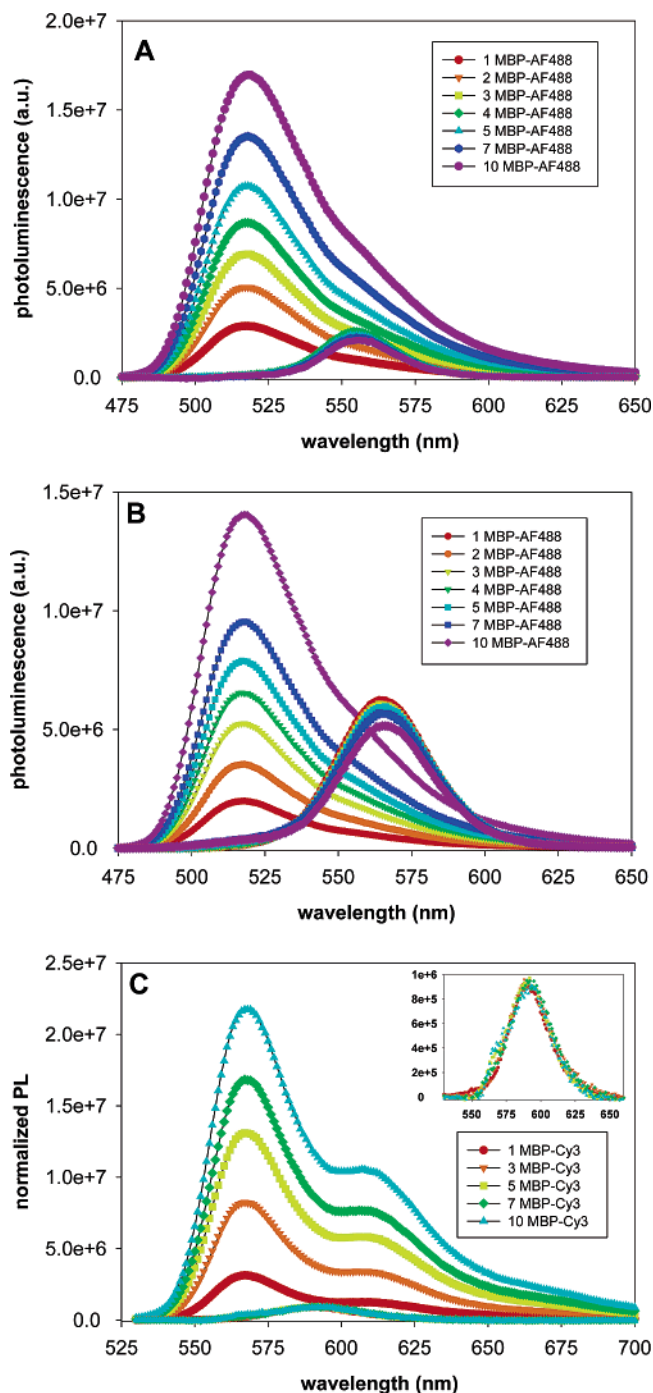


Figure 2. Photoluminescence spectra of the MBP–dye donor and the corresponding QD acceptor in dye–protein–QD nanoassemblies as a function of increasing dye to QD ratio for the three sets of donor–acceptor pairs studied. Signals were deconvoluted to show individual spectra for each fluorophore. Direct excitation of the QDs accounted for the entire acceptor signal in each case and was not subtracted. Control experiments using free MBP–dye were indistinguishable from the deconvoluted spectra shown for each conjugate. (A) AlexaFluor 488 dye (donor) and 555 nm emitting QDs (acceptor). (B) AlexaFluor 488 dye (donor) and 570 nm emitting QDs (acceptor). (C) Cy3 dye (donor) and 590 nm emitting QDs (acceptor); the 590 nm QD acceptor signal is shown in the inset to improve clarity.

a UV emission essentially identical to the one measured for the MBP–QD conjugates. This contrasts the finding reported in ref 13 where a 2-fold QD PL increase was implied.

Fluorescence Lifetime Measurements. Time-resolved fluorescence experiments can show changes in the exciton lifetime

(33) Lin, Z.; Cui, S.; Zhang, H.; Chen, Q.; Yang, B.; Su, X.; Zhang, J.; Jin, Q. *Anal. Biochem.* **2003**, *319*, 239–243.

(34) Born, M.; Wolf, E. *Principles of Optics*, 6th ed.; Pergamon Press: New York, 1986.

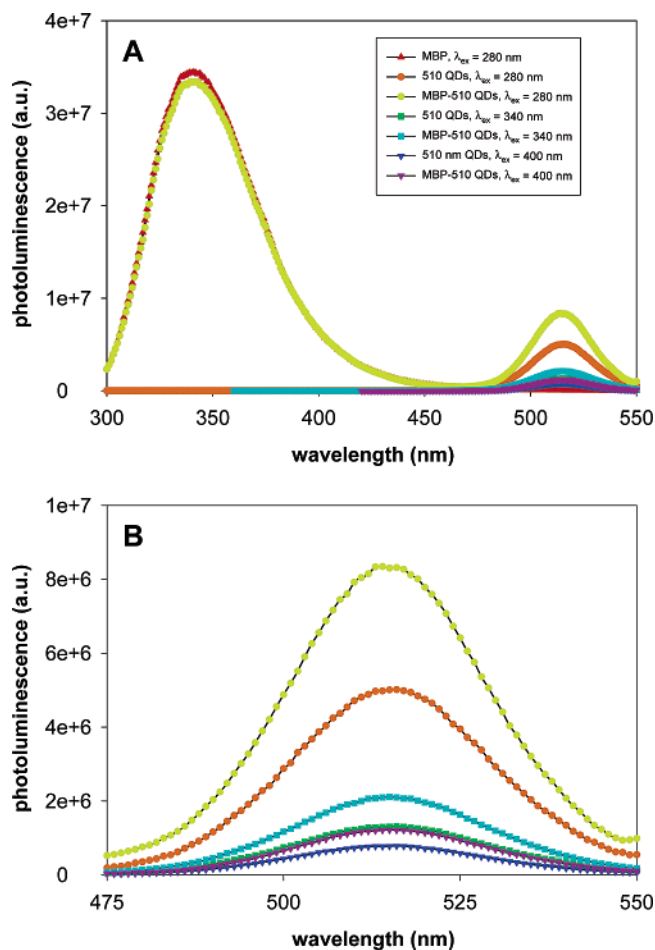


Figure 3. Fluorescence spectra showing MBP alone, 515 nm emitting QDs alone, and MBP-515 QD conjugates excited at various wavelengths. (A) PL spectra for MBP, 515 QDs, and MBP-515 QD conjugates measured at three excitation wavelengths (280, 340 and 400 nm). Samples containing MBP excited at 280 nm show characteristic PL emission from eight Trp residues per MBP molecule. Formation of the MBP-QD conjugate decreases the PL of MBP by less than 3% (i.e., within experimental error). (B) MBP-QD conjugates show an expected increase in QD PL compared to bare QDs due to coordination of the MBP at the QD surface (~66%, 62%, and 56% for 280, 340, and 400 nm excitation, respectively).^{4,5,23} MBP-QD conjugates excited at 280 nm do not show evidence of either decreased Trp PL or increased QD PL due to a potential FRET interaction between donor Trp and acceptor QDs.

of the donor molecule engaged in FRET with an acceptor molecule (brought in close proximity) and provide an independent verification of nonradiative exciton transfer. Combined with steady-state fluorescence results, measurements of exciton lifetime provide a critical test of whether nonradiative FRET between a donor and an acceptor pair occurs in a particular system. We have, for example, shown that in the format where a central QD donor was surrounded by several dye-labeled protein acceptors, a pronounced rate of FRET was measured, which led to a substantial loss of QD PL accompanied by a concomitant enhancement of the dye emission. The steady-state fluorescence results were confirmed by a pronounced shortening of the QD exciton lifetime with an increasing number of dye-labeled proteins assembled around the QD center in a QD bioconjugate.⁴ Decrease in the donor lifetime is one of the hallmarks of efficient FRET between organic dye molecules.²

In the present study, time-resolved fluorescence measurements were carried out using AF488–555 nm QD and Cy3–590 nm QD pairs. In each case, three samples consisting of dye-labeled

MBP, QDs conjugated to unlabeled MBP, and QD–dye-labeled MBP conjugates were used. For the AF488 and 555 nm emitting QD pair, fluorescence lifetimes were measured for five dye-labeled MBP-to-QD ratios, and compared to reference samples containing dye-labeled MBP or MBP-QD conjugates lacking dye labels, whereas only one ratio of 10 dye-labeled-MBP per QD was used for the Cy3–590 nm QD pair. Analysis of the lifetime data was complicated by the substantial overlap between the donor and acceptor emission spectra (see Figure 2A–C) and by the fact that the excitation laser source at 414 nm was near the valley of the absorption spectra of the dyes but well within the region where the extinction coefficient of the QDs is substantial. For the AF488–555 nm QD pair, donor lifetime was determined by integrating the measured intensity over a small wavelength interval (490–520 nm) within the blue edge of the emission where AF488 emission contribution is dominant and plotting the result as a function of delay time (at 0.25 ns intervals). Figure 4A shows a plot of the integrated AF488 signal as a function of delay time for several dye-to-QD ratios. The donor exciton lifetime τ_D was estimated by fitting the fluorescence decay curve to a biexponential function of the form $I_D(t) = \alpha_1 \exp(-t/\tau_1) + \alpha_2 \exp(-t/\tau_2) + I_B$, which provided an excellent fit to the data. Because neither pre-exponential factor was dominant (i.e., $\alpha_1 \approx \alpha_2$), both values were used to estimate an average donor lifetime using the relation $\bar{\tau} = \sum f_i \tau_i$, where $f_i = \alpha_i \tau_i / \sum \alpha_j \tau_j$, and average lifetime estimates are reported in Table 1.² For the Cy3–590 nm QD pair it was impossible to select a sizable spectral region (i.e., 20–40 nm window) where only the donor contribution is measured, due to significant overlap between the Cy3 and 590 nm emissions (Figure 2C). Figure 4B shows plots of the fluorescence signal decay versus time for MBP–Cy3, MBP–Cy3–590 nm QD conjugates, and 590 nm MBP–QD conjugates. The fluorescence signal for the MBP–Cy3–QD conjugates (squares in Figure 4B) was limited to the blue edge of the composite spectrum (PL integrated between 530 and 560 nm). Lines represent fits using the biexponential decay expression described above. The fit to the data for the MBP–Cy3–590 nm QD conjugates showed two clear contributions: a dominant dye contribution with a lifetime of 1.3 ns, nearly identical to the one measured for MBP–Cy3 only solution, and a longer less dominant QD contribution with a time constant of 8.6 ns, very close to the one measured for the MBP–QD conjugates (Figure 4B).

Figure 5A–D show time-resolved spectroscopic images of the fluorescence signals for the AF488–555 nm QD system following a short excitation pulse. Similar data were collected for the Cy3–590 nm QD pair (not shown), but with a more pronounced spectral overlap of the dye and dot contribution to the images as expected. In these images, the abscissa designates the wavelength, the ordinate designates the delay time (increasing downward), and intensity is depicted by color contours (increasing from blue to red). Figure 5A shows images from a solution containing dye-labeled proteins only for the equivalent concentration of 10 MBP–AF488 (no QDs present). Figure 5B shows the time series for a solution of the 555 nm QDs coated with 15 unlabeled MBP (no dye present). Figure 5C shows the time series for a solution of the MBP–QD conjugate where QDs are coated with 15 MBP, 10 of which are labeled with AF488. Figure 5D shows a superposition of the time series images collected from solutions of dye-labeled MBP only (Figure 5A) and 555 nm QDs only (Figure 5B). The superposed

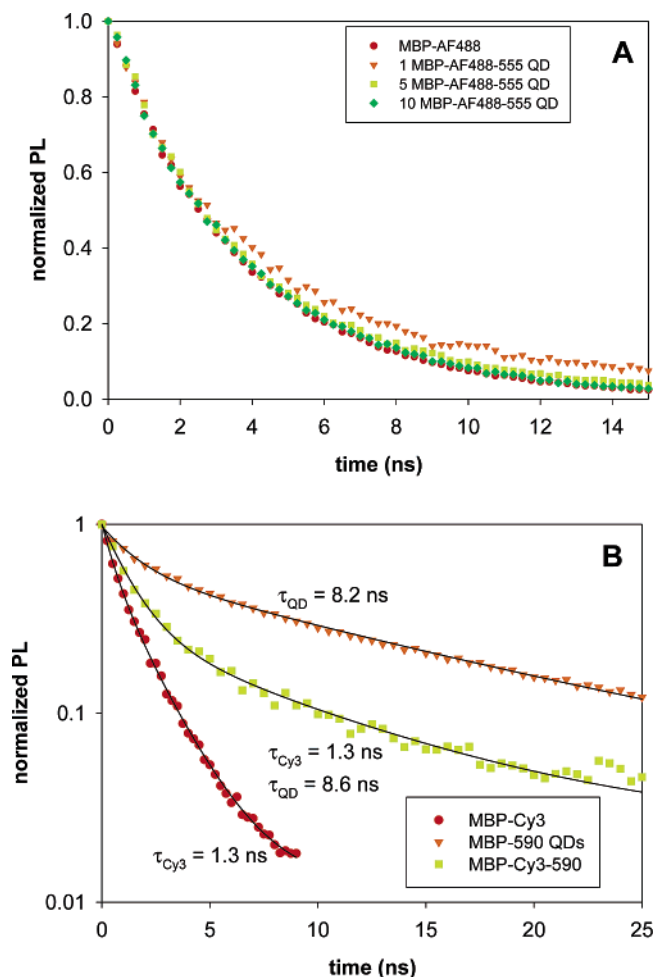


Figure 4. (A) Plot of the AlexaFluor 488 donor fluorescence intensity as a function of delay time following an excitation pulse. Data are shown for several nanoassemblies where the ratio of dye to QD is varied from 0 to 10 with the overall MBP to QD ratio fixed at 15. (B) Plots of the fluorescence intensity versus time for MBP–Cy3 (circles), MBP–Cy3–QD conjugates (squares), and MBP–QD (unlabeled protein) conjugates (triangles); only one labeling ratio was used. Due to the strong overlap between the Cy3 and 590 QD emissions, it was impossible to spectrally separate the dye contribution from that of the QDs in the composite intensity. Lines represent fits using a biexponential function as described in the text. The fit to the data for the MBP–Cy3–QD conjugates showed two distinct contributions: one from the Cy3 dye with a measured lifetime of 1.3 ns, almost identical to the one measured for the MBP–Cy3 only solution, and a QD contribution with a time constant of 8.6 ns, very close to the one measured for the MBP–QD sample.

set of images show a composite time–wavelength–intensity series for direct comparison with Figure 5C. In all images, the dashed lines mark the emission maxima of the two fluorophores, at 520 nm for AF488 and at 555 nm for the QDs. No change in the exciton lifetime could be measured. In fact, the data for the individual components extracted from the MBP–dye–QD conjugates are identical to those collected from solutions of the dye only or the QD only. These results complement and confirm the steady-state fluorescence data.

We now discuss the above findings and compare them to the predictions of the classical Förster formalism. The steady-state fluorescence data collected for the three sets of dye–QD pairs investigated, AF488–555 QDs, AF488–570 QDs, and Cy3–590 QDs consistently showed no evidence of nonradiative energy transfer between the dye donor and QD acceptor regardless of the dye–QD combination or the ratio of dye-labeled

Table 1. Measured Fluorescence Lifetimes, Quantum Yields, and Förster Distances for the Various Donor–Acceptor Pairs Used

fluorophore/conjugate	donor lifetime (ns)	donor QY	R_0 (Å)
MBP (Trp) ^a	0.5–3.1	0.13	
15 MBP (Trp)–510 QD ^b			37.2
MBP–Cy3	1.34 ± 0.07	0.20	
10 MBP–Cy3–590 QD	1.30 ± 0.07		50.9
MBP–AF488	3.36 ± 0.04	0.94	
1 MBP–AF488–555 QD	3.33 ± 0.15		66.0
3 MBP–AF488–555 QD	3.25 ± 0.19		
5 MBP–AF488–555 QD	3.46 ± 0.16		
7 MBP–AF488–555 QD	3.33 ± 0.14		
10 MBP–AF488–555 QD	3.35 ± 0.10		
MBP–AF488–570 QD			67.1
Ru–bpy–ITC	377 ± 18	0.04	
MBP–Ru–bpy–ITC	419 ± 15		
10 MBP–Ru–bpy–ITC–610 QD	160 ± 12		40.6

^a Data taken from ref 2. ^b Trp fluorescence present where $\lambda_{\text{ex}} = 280$ nm.

protein to QD. The characteristic changes in the photoluminescence properties that are commensurate with a FRET process are notably absent, namely there is no loss in donor PL or gain in acceptor emission following the dye–QD pair association due to conjugate self-assembly. Examination of the emission spectra after deconvolution of the composite signals indicate that the measured QD signal is constant within each set and is identical to the one generated from direct excitation of the QD solution in the absence of acceptor dyes (i.e., control sample), independent of the number of dye donors present in each QD conjugate for all three pairs studied. As expected, emission due to direct excitation increased with increasing nanocrystal size (or maximum emission wavelength) for the 555 and 570 nm emitting QDs, since QD absorption at the excitation line increases with increasing nanoparticle size (Figure 2A and B).¹² The weaker signal exhibited by the 590 QDs was due to excitation at 520 nm rather than 450 nm (see Figure 2C). Similarly, the donor dye signals were found to proportionally increase with increasing dye to QD ratio and were unaffected by the presence of the proximally positioned QDs (Figure 2A–C). Similarly the data shown in Figure 3 indicate that there is no measurable FRET between the Trp and the QDs despite the large number of potential Trp donors in the MBP–QD conjugate.

The above steady-state fluorescence results were further complemented and confirmed by the time-resolved fluorescence data shown in Figures 4 and 5. These experiments indicate that there is no change in the AF488 or Cy3 donor lifetime as a result of interactions with the central QD once QD–protein conjugates are formed. Further, the AF488 lifetime (Table 1) essentially remains constant when the number of donors arrayed around the QD surface is systematically increased. The data shown in Figures 5C and 5D indicate that the time series collected for the individual MBP–AF 488 and 555 QDs match exactly the data for the composite spectrum collected for the QD–dye-labeled protein bioconjugates. Absence of any measurable change in the exciton lifetime of the donor upon interaction with the proximal QD located in the center of the conjugate is the most conclusive evidence that there was no measurable FRET between the dye and QD donor–acceptor pair used in the present investigation.

The results shown here are *a priori* surprising given the favorable degree of spectral overlap for these three sets of dye–QD pairs used (see Figure 1). Absence of FRET can neither be attributed to a lack of conjugate formation nor to a prohibitively large separation distance between the donor and acceptor centers in the present set of QD–dye-labeled protein complexes. MBP–

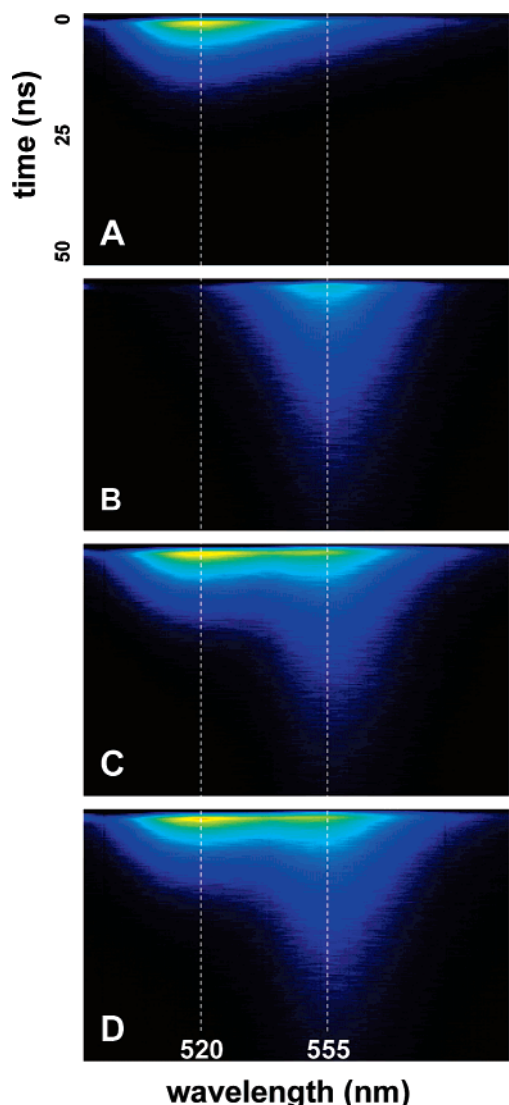


Figure 5. (A) Time–wavelength–intensity plot showing the PL decay of AlexaFluor 488 donor as a function of delay time after an excitation pulse. Intensity is shown as color contours. Sample concentration is equivalent to 10 MBP–AF488 per QD (no QDs present in this sample). (B) A similar plot showing the PL of 555 nm emitting QD acceptors coated with 15 unlabeled MBP. (C) Plot showing the PL intensity of the conjugate nanoassembly comprised of 555 nm emitting QDs with 5 MBP/10 MBP–AF488. (D) Plot created by adding together the images shown in plots A and B. Note that the images shown in plots C and D are indistinguishable which indicates lack of substantial nonradiative interaction within the conjugate.

QD conjugation via histidine–Zn coordination using DHLA-capped QDs has been verified in a variety of assays.^{4,5,9} Furthermore, our self-assembled conjugates produce QD-to-dye center-to-center separation distances of ~ 70 – 75 Å, well within efficient FRET range.^{4,5,32} Calculated Förster distances, R_0 , derived from the experimental absorption and PL data (shown in Figure 1) are 66 Å for AF 488 and 555 nm QD pair, 67 Å for AF 488 and 570 nm QD pair, and 51 Å for Cy3 and 590 nm QD pair; they are smaller for Trp–515 nm QD pair (~ 37 Å). These values imply that, with the above separation distance of 70–75 Å and a configuration where multiple energy donors interact with a single acceptor, a substantial rate of FRET would result (in particular for the MBP–dye–QD case), as predicted by the Förster formalism. The immobilization of several donor molecules around the QD acceptor center, which should enhance

the rate of FRET to QD acceptors, had no beneficial effects. These data contrast with results obtained using an analogous format where QDs served as energy donors to dye-labeled MBP acceptors.⁴ A pronounced change in the PL signals of both QD and dye was measured for increasing MBP–dye to QD ratios and correlated with a substantial shortening of the donor exciton lifetimes in that format. Yet the Förster distances measured in those FRET experiments were smaller than those present in this investigation.⁴ Taken together, these results strongly suggest that even though a pronounced rate of nonradiative FRET was measured and successfully analyzed within Förster formalism in the configuration when QDs functioned as energy donors to dye-labeled protein acceptors, no measurable energy transfer could be observed in the reverse format where these same QDs serve as energy acceptors to dye donors. This was regardless of the number of donors surrounding the central QD acceptor and whether an organic dye or the naturally occurring Trp was used as an energy donor.

The present findings may however be explained within the framework of an effective competition among radiative, non-radiative, and FRET decay channels (or rates) of the donor excitation energy following absorption of a higher energy photon. This is due to a considerable difference between the exciton radiative decay lifetimes of the donor and acceptor, τ_D and τ_A , respectively. This process is further complicated by the rather large extinction coefficients of both donor and acceptor at the excitation line (see Figure 1). In a FRET system, when the donor absorbs a high-energy photon, an electron is excited into the LUMO (for an organic dye molecule) or the conduction band (for a semiconductor QD), and the exciton relaxes via three competing pathways. The first pathway is radiative with a characteristic lifetime τ_D and should result in the emission of a photon characteristic of the donor molecule (i.e., no FRET occurs). The second pathway is nonradiative FRET with a characteristic time τ_{FRET} and results in the transfer of the excitation energy to the acceptor, which then relaxes radiatively and emits a lower energy photon characteristic of the acceptor fluorophore. The third pathway is also nonradiative where energy is dissipated without being transferred to the acceptor. In this case, the FRET decay channel effectively competes with the radiative and nonradiative channels. Efficient FRET requires the presence of ground state acceptors with a substantial energy overlap in close proximity to an excited donor for rapid transfer of the excitation energy before the donor decays radiatively or nonradiatively. In the present system, the radiative decay rates of the dye donors are about 2–10 times faster than those of QD acceptors, while the extinction coefficient is about an order of magnitude larger for the QDs ($\tau_A \approx (2 - 10)\tau_D$ and $\epsilon_A \approx 10\epsilon_D$). This generates a configuration where the QD acceptors are more efficiently excited by direct excitation than the individual donor molecules. The excited QDs cannot rapidly return to the ground state and efficiently receive energy via FRET. Externally charged or optically excited QDs should have lower probability to absorb a second excitation energy. In particular, the Guyot–Sionnest group reported that injection of an electron in the lowest quantum-confined state of the conduction band of CdSe and CdSe–ZnS nanocrystals, by mixing the QDs with strong redox molecules in a solid sample, leads to bleaching of the first interband (over the band gap) exciton transition, a strong mid-infrared intraband absorption, and a quenching in the photoluminescence emission.^{35,36} Further, if an excited QD receives an additional excitation energy (e.g.,

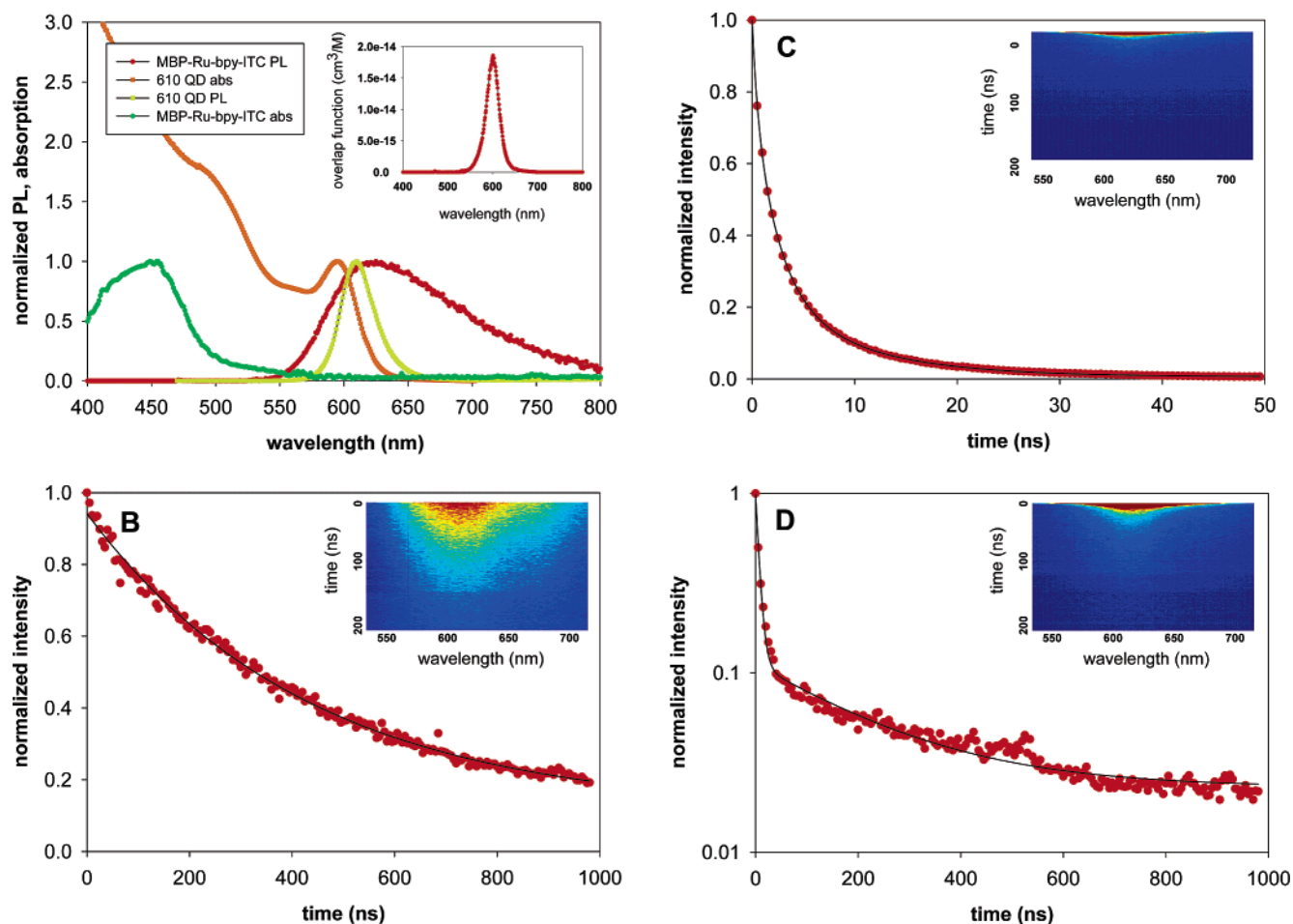


Figure 6. (A) Absorption and PL spectra for both MBP–Ru-bpy-ITC dye and 610 nm emitting QDs used. The experimental overlap function for the pair is shown in the inset. (B–D) Fluorescence intensity plotted as a function of delay time following a short excitation pulse: (B) MBP–Ru-bpy-ITC alone, (C) MBP–610 QDs alone, (D) MBP–Ru-bpy-ITC–610 QD conjugate. The inset is a time–wavelength–intensity plot for each sample where the false color intensity scale is the same among all three plots. As shown in plot D, two distinct contributions can be isolated due to the relatively short lifetime QDs and long lifetime Ru-bpy-ITC. The short decay time determined by the fitting procedure is identical to the one for the MBP–QD only sample, whereas the longer decay time is about half of the lifetime found for MBP–Ru-bpy-ITC alone. A pronounced decrease in the donor lifetime provides evidence of FRET in this conjugate.

via FRET), this can increase the rate of Auger recombination/ionization and reduce the probability of acceptor emission via radiative channels.^{27,37,38} These two phenomena would create a set of QD acceptors that are still excited and affected by Auger recombination on a time scale of donor radiative relaxation. This will ultimately make the direct radiative (or nonradiative) decay channel the dominant and only relaxation mechanism of the excitation energy at the expense of any FRET process.

The above rationale can also be discussed using the following expression for the rate of FRET (k_{FRET}) derived using the various lifetimes:²

$$\tau_{\text{DA}} = 1/(k_{\text{FRET}} + \tau_{\text{D}}^{-1}) \text{ or } k_{\text{FRET}} = \tau_{\text{DA}}^{-1} - \tau_{\text{D}}^{-1} = \frac{\tau_{\text{D}} - \tau_{\text{DA}}}{\tau_{\text{D}}\tau_{\text{DA}}} \quad (1)$$

where τ_{D} and τ_{DA} designate the exciton lifetime of the isolated donor and the donor interacting via FRET with a proximal acceptor, respectively. Equation 1 implies that a substantial FRET interaction between a donor and an acceptor could only result in a shortening of the donor lifetime ($\tau_{\text{DA}} < \tau_{\text{D}}$), which in turn can be realized only when using a donor–acceptor pair that has comparable radiative decay lifetimes (or comparable

decay rates). Any other configuration would produce an unphysical negative value for k_{FRET} if τ_{DA} exceeds τ_{D} .

FRET between QDs of different size (or band edge absorption) has been reported in several studies.^{39,40} This does not contradict the above rationale, since QD donors and QD acceptors have comparable lifetimes. In this case nonradiative energy transfer from a smaller size QD (higher energy band gap) to a larger size QD (lower energy band gap) competes more effectively with the radiative channel; it is further facilitated by a lower probability for Auger ionization, since the equally excited QD acceptors are able to relax at time scales comparable to those for the radiative pathways of the smaller size QD donors.

To test the validity of our rationale and the importance of the exciton lifetimes on the rate of FRET, we carried out additional experiments using a prefunctionalized ruthenium

- (35) Shim, M.; Guyot-Sionnest, P. *Nature* **2000**, *407*, 981–983.
 (36) Wang, C. J.; Shim, M.; Guyot-Sionnest, P. *Science* **2001**, *291*, 2390–2392.
 (37) Efros, A. L.; Rosen, M.; Kuno, M.; Nirmal, M.; Norris, D. J.; Bawendi, M. G. *Phys. Rev. B* **1996**, *54*, 4843–4856.
 (38) Htoon, H.; Hollingsworth, J. A.; Dickerson R.; Klimov, V. I. *Phys. Rev. Lett.* **2003**, *91*, 227401.
 (39) Kagan, C. R.; Murray, C. B.; Bawendi, M. G. *Phys. Rev. B* **1996**, *54*, 8633–8643.
 (40) Achermann, M.; Petruska, M. A.; Crooker, S. A.; Klimov, V. I. *J. Phys. Chem. B* **2003**, *107*, 13782–13787.

chelate dye Bis(bipyridine)-5-(isothiocyanatophenanthroline)-Ru(PF₆)₂, Ru-bpy-ITC (Sigma-Aldrich, St. Louis, MO), which has a reported long phosphorescent radiative lifetime of 350 ns, to label MBP.⁴¹ The Ru-bpy-ITC dye has a broad emission maximum around 625 nm and a maximum absorption at 454 nm (Figure 6A); it was chosen from among other available Ru-bpy dyes because its emission was the most compatible with our largest QDs having their emission centered around 610 nm. The Ru-bpy-ITC was conjugated to MBP by reacting the isothiocyanate group with the epsilon amine of lysine residues, as described previously.⁷ Amino reactive dyes preferentially label the Lys141, 143, 145 residues of MBP.⁷ UV-vis absorption confirmed a dye to protein ratio of ~1.5. Ru-bpy-ITC-labeled MBPs were immobilized on 610 nm emitting QDs and used for both steady-state and time-resolved fluorescence experiments. Ru-bpy-ITC has a poor PL quantum yield (~0.04) and resulted in a modest Förster distance, R_0 , of ~40 Å with the present red-emitting QDs.

Steady-state fluorescence experiments were inconclusive, due to the pronounced degree of spectral overlap between the PL of the dye and QD pair and the strong signal generated from the direct excitation contribution of the acceptor. However, time-resolved fluorescence experiments carried out using the same time gated setup described above and excitation at 414 nm indicate that there is a substantial rate of FRET, reflected in a shortening of the Ru-bpy-ITC exciton lifetime compared to the one measured for unconjugated Ru-bpy-ITC-labeled MBP (see Figure 6B–D). The measured excited-state fluorescence lifetimes for the MBP–Ru-bpy-ITC and Ru-bpy-ITC alone were 419 ± 15 ns and 377 ± 18 ns, respectively (see Table 1). The value for Ru-bpy-ITC is slightly larger than the 350 ns reported by the manufacturer for soluble free dye.⁴¹ Changes in the fluorescence properties of dyes once attached to the proteins compared to free dyes are commonly observed, and the larger lifetime value measured for MBP–Ru-bpy-ITC agrees with that.² Analysis of the time-resolved data for the conjugates was complicated by the pronounced overlap of the QD and dye PL signals; however, data analysis benefited from the pronounced difference between the lifetimes of the two fluorophores ($\tau_{\text{QD}} \ll \tau_{\text{Ru}}$), and accurate individual time constants for QDs and Ru-bpy-ITC were deduced from the experimental data. We extracted a fast component with a time constant of $\sim 7 \pm 1$ ns and a much slower contribution with a time constant of $\sim 160 \pm 12$ ns, which were attributed to QD and MBP–Ru-bpy-ITC, respectively. Further, the short time constant is identical to the one measured for a QD only sample. These findings indicate that there is little or no change in the QD exciton lifetime but a substantial shortening of dye excitation lifetimes after QD–dye-labeled MBP conjugate formation compared to the values extracted for the free fluorophores. Nonetheless, since average QD lifetimes have been reported to vary anywhere between 3 and 15 ns depending on the sample, size distribution, surface capping, and the time resolution afforded by the experimental setup, we consider any change smaller than those limits not strong enough to draw any solid conclusion based on changes in the acceptor lifetime. However, the change in the dye donor lifetime is much more pronounced (and far exceeds experimental uncertainties), which implies that a substantial rate of FRET was observed with the present donor–acceptor pair. This provides strong evidence to our rationale based on competition

between radiative decay and FRET decay channels to explain our present results. Absence of conclusive proof of FRET in the steady-state data despite the pronounced rate expected from the lifetime data can be attributed to the poor PL quantum yield of the donor combined with the high degree of direct excitation of the acceptor, which in this case could make deducing a FRET efficiency as high as 50% using changes in donor PL difficult to detect when using average and integrated ensemble fluorescence experiments. This is only one factor that intervenes as other processes, such as the pronounced direct excitation of the QD acceptor in the region where dyes are excited, could still interfere with the FRET process and its efficiency. These findings although promising are still not entirely conclusive. Additional experiments using other systems and better metal chelate dyes will be attempted to derive more conclusive information of the effectiveness of using luminescent QDs as energy acceptors in QD–dye-labeled protein conjugates.

Conclusions

We have examined the use of luminescent CdSe–ZnS QDs as energy acceptors in FRET-based assays with organic dyes as energy donors in QD–dye labeled protein conjugates. Organic dyes were covalently attached to a specific residue within engineered MBP sequences and self-assembled on the QD surface to create dye-labeled proteins immobilized on the QD surface with a given donor–acceptor separation distance. Three pairs of dyes and QDs were employed to examine the effects of spectral overlap, donor lifetime, and the number of donor molecules surrounding a centrally located single QD acceptor. We measured steady-state and time-resolved fluorescence and found that both sets of experiments clearly indicate that there is no evidence of FRET between the dyes and QDs, independent of the dye–QD pair and the QD–dye-labeled protein conjugate configuration. We attributed these findings to an effective competition between the fast radiative decay channels of the donor dye and slower nonradiative FRET decay pathways; this is due to a relatively longer exciton lifetime of the QD acceptor compared to that of the donor. This process is further exacerbated by the strong direct excitation of the QDs, due to their rather broad and large extinction coefficient spectra, which in turn can make Auger recombination more effectively compete with FRET decay channels in such a system.

The rationale based on the competition between radiative decay and FRET decay channels was tested using a metal chelate ruthenium complex dye with a long phosphorescent lifetime that was attached to the protein and conjugated to the QDs. Preliminary time-resolved fluorescence data confirm our findings, with an observed substantial shortening of the dye excitation lifetime upon QD–ruthenium dye–MBP conjugate formation.

Acknowledgment. We thank Dr. Marcel Bruchez, Jr. from QD Corporation for the fruitful discussions and useful suggestions. A.R.C. and I.L.M. acknowledge National Research Council Fellowships through the Naval Research Laboratory. H.M. thanks K. Ward and A. Ervin at the Office of Naval Research (ONR) for research support, Grant No. N001404WX20270. B.R.F. acknowledges the National Defense Science and Engineering Graduate Fellowship Program for support.

JA045676Z

(41) Terpetsching, E.; Szmajcinski, H. M.; Lackowicz, J. R. *Biophys. J.* **1995**, *68*, 342–350.